

**This item is the archived peer-reviewed author-version of:**

In situ electron diffraction tomography using a liquid-electrochemical transmission electron microscopy cell for crystal structure determination of cathode materials for Li-Ion batteries

**Reference:**

Karakulina Olesia, Demortiere Arnaud, Dachraoui Walid, Abakumov Artern M., Hadermann Joke.- In situ electron diffraction tomography using a liquid-electrochemical transmission electron microscopy cell for crystal structure determination of cathode materials for Li-Ion batteries

Nano letters / American Chemical Society - ISSN 1530-6984 - 18:10(2018), p. 6286-6291

Full text (Publisher's DOI): <https://doi.org/10.1021/ACS.NANOLETT.8B02436>

To cite this reference: <https://hdl.handle.net/10067/1547500151162165141>

*In situ* electron diffraction tomography using a  
liquid-electrochemical TEM cell for crystal structure  
determination of cathode materials for Li-ion  
batteries

*Olesia M. Karakulina,† Arnaud Demortière,\*‡,§ Walid Dachraoui,§*

*Artem M. Abakumov||, Joke Hadermann\*,†*

†EMAT, University of Antwerp, Groenenborgerlaan 171, B-2020 Antwerp, Belgium

‡Réseau sur le Stockage Electrochimique de l'Energie (RS2E), CNRS FR 3459, 80039 Amiens,  
France

§Laboratoire de Réactivité et de Chimie des Solides (LRCS), CNRS UMR 7314 – Université de  
Picardie Jules Verne, 80039 Amiens, France

||Skoltech Center for Electrochemical Energy Storage, Skolkovo Institute of Science and

Technology, 143026 Moscow, Russian Federation

**Keywords:** Liquid TEM, electron diffraction tomography, *in situ* electrochemical TEM, structural determination, LiFePO<sub>4</sub> cathode materials

## ABSTRACT

We demonstrate that changes in the unit cell structure of lithium battery cathode materials during electrochemical cycling in liquid electrolyte can be determined for particles of just a few hundred nanometer in size, using *in situ* transmission electron microscopy (TEM). The atomic coordinates, site occupancies (including lithium occupancy) and cell parameters of the materials can all be reliably quantified. This was achieved using electron diffraction tomography (EDT) in a sealed electrochemical cell, with conventional liquid electrolyte (LP30) and LiFePO<sub>4</sub> crystals, which has a well-documented charged structure to use as reference. ~~The structure refined for the charged LiFePO<sub>4</sub>, i.e. FePO<sub>4</sub>, corresponds well to literature data.~~ *In situ* EDT in a liquid environment cell provides a viable alternative to *in situ* X-ray and neutron diffraction experiments, due to the more local character of TEM, allowing to obtain single crystal diffraction

data from multiphased powder samples and from sub-micron sized to nanometer sized particles. EDT is the first *in situ* TEM technique to provide information at unit cell level in liquid environment of a commercial TEM electrochemical cell. Its application to a wide range of electrochemical experiments in liquid environment cells and diverse types of crystalline materials can be envisaged.

The development of efficient Li-ion batteries is vital for transforming our energy-greedy society to one that is more sustainable, where renewable energy will be efficiently stored and widely used<sup>1</sup>. So far, Li-ion batteries are mainly used in portable electronic devices.<sup>2,3</sup> However, there is an increasing demand for powering electrical vehicles and stabilizing the fluctuation of renewable energy production, necessitating an optimization of electrochemical energy storage focused on these applications. Ideally, for rechargeable and long-lasting batteries, the electrode materials should be able to reversibly (de)intercalate Li-ions.<sup>4</sup> Consequently, the active positive electrode (cathode) materials of Li-ion batteries are commonly inorganic compounds with Li-ions residing in voids of a framework or between layers, consisting of transition metals coordinated by oxygen, often combined with polyanion groups, such as phosphates or sulfates.<sup>3,5</sup>

Upon charging the battery, Li<sup>+</sup> ions move from the cathode material to the anode material through the electrolyte, whereas the transition metal atoms and, partly, oxygen atoms in the cathode structure get oxidized to retain the charge balance<sup>3</sup>. During discharge, the Li<sup>+</sup> ions are reintroduced into the cathode<sup>3</sup>. This process can result in significant transformations of the cathode's structure while trying to accommodate the changing conditions, such as migration of transition metals, loss of oxygen or rearrangements of the metal-oxygen polyhedra.<sup>5-9</sup> It is crucial to know which structural changes occur at unit cell level, in order to understand the evolution of the electrochemical performance and degradation routes of the different cathode materials. During the last decade new *in situ* and *operando* analytical tools have been developed to monitor structural and chemical transformations, resulting in important advances in the knowledge on electrochemical energy storage.<sup>10-13</sup> For *in situ* tracking of structural changes, currently X-ray (XRD) and neutron powder diffraction (ND) are typically applied.<sup>10,14</sup> Using *in situ* transmission electron microscopy (TEM), dynamic processes during battery operation can be visualized in

real time and with high spatial resolution,<sup>15–18</sup> however, not yet at atomic resolution when using a liquid electrolyte environment. *In situ* electron diffraction has not been used yet for structure determination within electrochemical cells. This technique has a very important advantage: it can probe crystalline matter at a more local scale than powder X-ray and neutron diffraction. This allows getting single crystal diffraction information from nanoparticles<sup>19</sup> and multi-phased bulk samples<sup>20</sup>.

Sealed liquid cells for TEM emerged twenty years ago and gradually became more complex, with the integration of biasing devices to perform electrochemical measurements (Figure 1, a).<sup>10,21–25</sup> They permit the observation and analysis of battery processes at nanoscale in liquid high-vapor conventional electrolytes.<sup>26</sup> So far, the *in situ* experiments were mostly dedicated to imaging either in TEM or scanning TEM (STEM) modes.<sup>21,26</sup> Due to the presence of the electrodes and a polymer protection layer avoiding extra reactions out of the observation window, the minimal space between the windows in currently available commercial cells is 500 nm. When filled with liquid, the windows bend outwards, creating an even thicker liquid layer.<sup>27</sup> As a result, it is not possible to image the crystal structure with atomic resolution as can be done in a non-electrochemical liquid environment cell where the space between the windows can be decreased to 50 nm.<sup>27–33</sup> In this paper, we demonstrate that *in situ* electron diffraction tomography in a Protochips electrochemical TEM cell can, on the contrary, give atomic-level information on the structural changes of cathode materials upon cycling with conventional liquid electrolyte.

Electron diffraction tomography (EDT) was developed by Kolb *et al.*<sup>19,34</sup> to decrease the multiple scattering effects in electron diffraction experiments and enable the quantitative use of the measured reflection intensities within the kinematical approximation (*i.e.* assuming single

electron scattering), as is preferable for structure solution. EDT is based on the acquisition of a series of off-zone electron diffraction patterns by tilting a crystal around a single axis (Figure 1, b). The off-zone character reduces the number of multiple scattering paths for the electrons. The individual electron diffraction patterns (two-dimensional sections of the reciprocal lattice of the crystal) are then combined with a reconstruction process into a three-dimensional collection of reflections with their intensities. This method has already proven successful for the solution and refinement of numerous crystal structures.<sup>20,35–41</sup> The method was also already used for the *ex situ* structure determination of cathode materials after electrochemical cycling, allowing to detect the Li positions and refine their occupancy and to solve structures of unknown delithiated phases.<sup>9,42,43</sup> However, so far, EDT was only used in the vacuum environment of the conventional TEM setup. In this paper, we demonstrate that *in situ* EDT in an electrochemical cell with conventional liquid electrolyte (1.0 M LiPF<sub>6</sub> EC/DMC (1:1) (LP30)) reveals lattice parameter variations and changes in the crystal structure, including all atomic coordinates and occupancies, even for the Li position. For this proof-of-concept, we use the well-studied and commercially deployed material LiFePO<sub>4</sub>.<sup>44</sup>

LiFePO<sub>4</sub> was synthesized by hydrothermal method followed by carbon coating (see Supporting Information).<sup>43</sup> The *in situ* EDT study was performed using a Protochips Poseidon electrochemical TEM holder filled with 1.0 M LiPF<sub>6</sub> EC/DMC (1:1) (LP30) electrolyte. The pristine and *in situ* charged materials were investigated in two separate cells, to reduce the effect of beam irradiation during this first demonstration experiment. We discuss below how, in future experiments, the same crystal can be followed throughout the charge-discharge cycle in a single cell. The electron diffraction patterns were recorded using a CMOS camera OneView from Gatan (30fps at 2k × 2k), because a conventional CCD camera provided insufficient quality of

the pattern (Figure 2, a-b). More details about sample preparation and experimental setup are given in the Supporting Information.

The minimum thickness of electrochemical cell provided by Protochips is 500 nm. Due to the difference in pressure between the fluid within the cell (1 atmosphere) and the vacuum in the microscope column ( $10^{-9}$  Torr), the silicon nitride windows bend outwards, increasing the thickness up to 1  $\mu\text{m}$  in the middle of the window.<sup>27</sup> In literature, electron diffraction was observed for cells with 130-500 nm space between the windows, with water based solutions.<sup>31,32</sup> In case of thicker cells, no reflections could be observed due to scattering of the electron beam by the liquid. For such cells, electron diffraction was reported only after accidental vaporization of water by radiolysis and heat until only a thin liquid layer was left.<sup>30</sup> Indeed, also in our experiment, reflections could be observed only after reducing the liquid thickness by evaporating or/and depleting part of the liquid, leaving a thin liquid layer around the crystals and top and bottom inside surfaces of the chip due to wetting (Figure 1).<sup>45,21</sup> We verified the presence of the remaining liquid using electron energy loss spectroscopy (Figure S3).

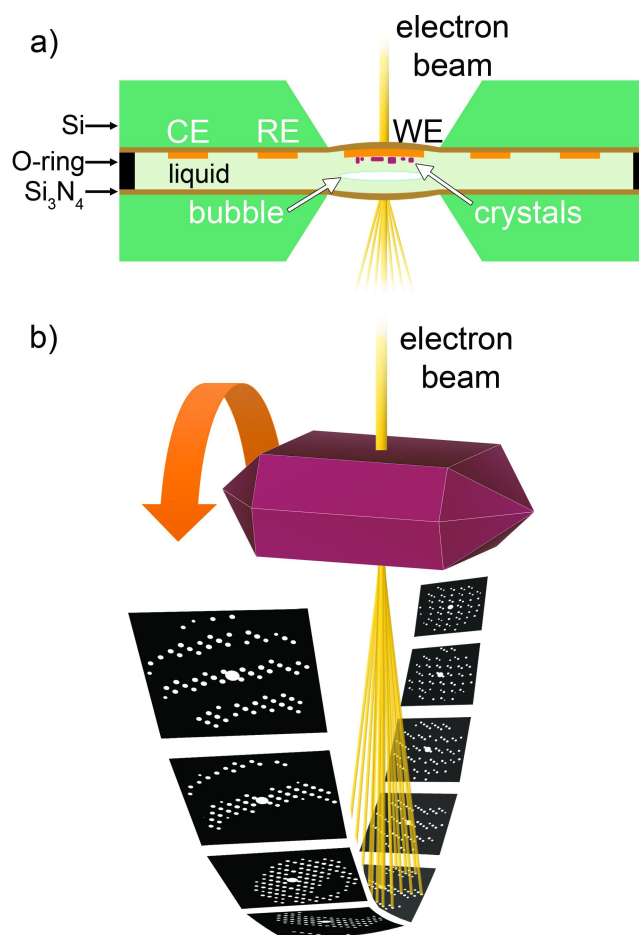


**Figure 1.** (a) Schematic side-view cross section of the *in-situ* electrochemical cell. The cell contains a working electrode (WE), counter electrode (CE) and reference electrode (RE). The crystals are stuck to the WE, which is made of electron-transparent glossy carbon. (b) Representation of the electron diffraction tomography concept.

The tomography series was acquired manually, obtaining electron diffraction patterns  $1^\circ$  apart over a total range of  $60^\circ$  (maximal possible tilt with the specific holder used in a FEI Tecnai microscope with Super-Twin pole pieces). For the pristine sample, only  $35^\circ$  of this tilt were used, discarding patterns that were obviously obtained after the crystal had been displaced, probably

due to fluid movement induced by rotation of the cell. Under an intense electron beam, the organic electrolyte decomposed, forming solid amorphous contamination. The precise nature of the contamination is out of scope of the current paper. To avoid this contamination, it is necessary to use short exposure times and short intervals between exposures, however, longer exposure times give a better signal-to-noise ratio. Balancing the two resulted in our case in an 8 second acquisition time per pattern using a very weak beam intensity and dose ( $10 \text{ e}^-/\text{nm}^2\text{s}$ ). On the resulting electron diffraction patterns, clear and sharp reflections are seen (Figure 2, a). The 3D reconstruction of the reciprocal space shows sphere-like intensity domains indicating good quality tomography data and 3D reconstruction (Figure 2, b, c).

Up to 582 reflections were collected with  $I > 1\sigma(I)$  (Table S1). The PETS software was used to analyze the data and make the 3D reconstruction.<sup>46</sup> The crystal structure was refined using Jana2006 software.<sup>47</sup>

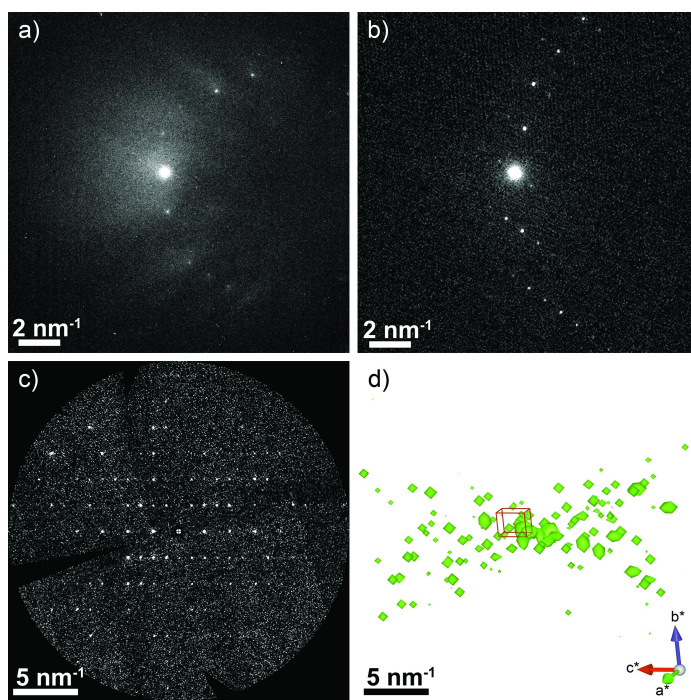


**Figure 2.** *In situ* electron diffraction in liquid electrolyte (1.0 M LiPF<sub>6</sub> EC/DMC (1:1) (LP30)) obtained using (a) a regular CCD camera (b) a CMOS camera (similar orientation, similar conditions as in (a)). (c) *h0l* section of the reconstructed reciprocal lattice. (d) Complete reconstructed reciprocal lattice.

The cell parameters of LiFePO<sub>4</sub> and FePO<sub>4</sub> were in agreement with literature (accuracy better than 1.3%) (Table 1)<sup>44</sup>. In case of FePO<sub>4</sub>, the full angular range of 60° could be used and the accuracy was even better than 0.5%. This shows that as a first step, the evolution of unit cell parameters upon electrochemical cycling can be tracked in *in situ* liquid electrochemical cells.

**Table 1.** Cell parameters for the pristine sample, LiFePO<sub>4</sub>, and the charged sample, FePO<sub>4</sub>.

Phase	Method	a, Å	b, Å	c, Å	Accuracy, %			Ref.
					a	b	c	
LiFePO <sub>4</sub>	XRD	10.3298(3)	6.0049(2)	4.6936(2)				*
	EDT	10.198(6)	6.016(2)	4.752(2)	1.3	0.1	1.2	*
	Neutron	10.3333(3)	6.0095(2)	4.6949(1)				1
FePO <sub>4</sub>	EDT	9.840(3)	5.742(4)	4.779(2)	0.4	0.5	0.1	*
	Neutron	9.823(2)	5.786(1)	4.784(1)				1

\*Experimental data

The quality of the electron diffraction tomography series was sufficient to perform *ab initio* solution of the crystal structures of LiFePO<sub>4</sub> and FePO<sub>4</sub>. The atom positions were obtained using the charge flipping algorithm as implemented in Superflip.<sup>48</sup> For both the pristine and the charged material, the Fe, P and O positions were correctly located, with less than 0.01 difference in the relative coordinates compared to those in literature. The oxygen positions were further refined using soft constraints on the P-O interatomic distances. The refined positions of the Fe, P and O atoms were in agreement with those refined from our own powder XRD data (pristine

material) and with the literature data (pristine and charged) (Table S4-7). The reliability factor is around 30%, which is acceptable for refinements based on electron diffraction tomography data, where the intensities are treated as due to single scattering events. (Table S1).<sup>20</sup> At this point, the Li positions still needed to be added to the structure.

The Li position in LiFePO<sub>4</sub> was detected using the difference Fourier map of the electrostatic potential. In Figure 1, a positive peak can be seen at the (0.5, 0, 0.5) position (Figure 3, b), corresponding to the Li position (*4a*: 0.5, 0, 0.5) according to literature. After adding Li in this position, the refined Li occupancy was 1.1(2). In case of FePO<sub>4</sub> (Figure 3, c), this peak was not observed, showing that Li was effectively removed from the structure.

The average Fe-O distance shrinks from 2.18Å in LiFePO<sub>4</sub> to 2.03Å in FePO<sub>4</sub> in accordance with oxidation of Fe<sup>2+</sup> (*r* = 0.78Å) to Fe<sup>3+</sup> (*r* = 0.65Å) upon full Li extraction. This corresponds to a change in bond valence sum for Fe from 1.91 for LiFePO<sub>4</sub> to 3.15 in FePO<sub>4</sub>, indicating that the refined structures are chemically sensible.

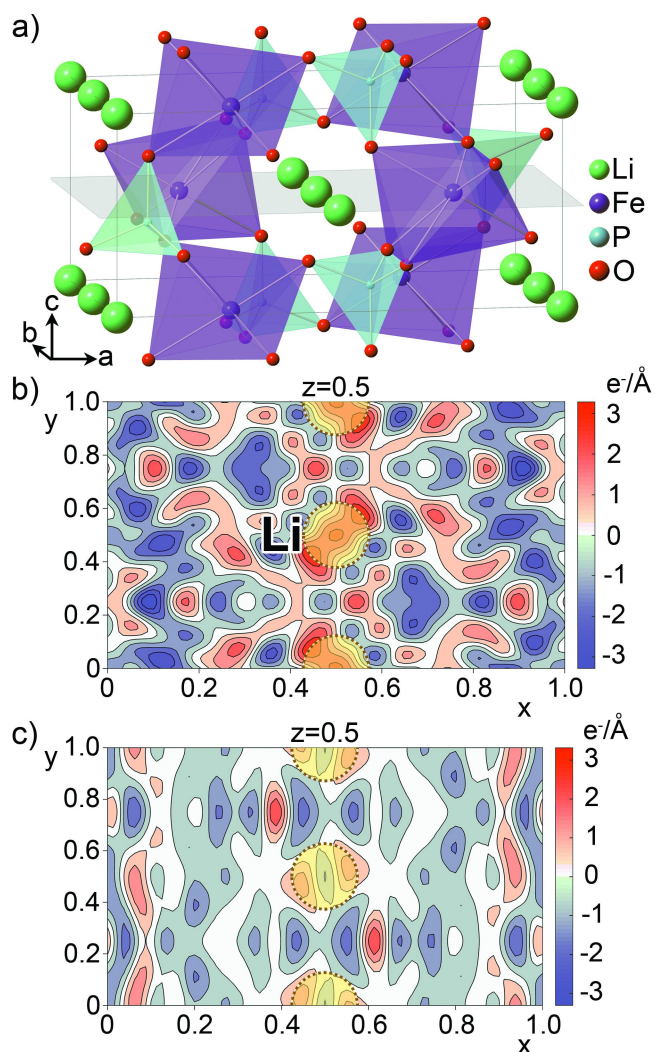


**Figure 3.** The crystal structure of  $\text{LiFePO}_4$  (a). Difference Fourier maps of scattering density for the section marked by the grey plane in (a), for  $\text{LiFePO}_4$  (b) and  $\text{FePO}_4$  (c) before inclusion of any Li atoms to the structure refinement. A pronounced peak of scattering density indicates the presence and location of Li in  $\text{LiFePO}_4$  (position indicated with a yellow disk). In  $\text{FePO}_4$  the positive peak is absent.

These results demonstrate that it is possible to solve and refine the crystal structure of electrode materials from data obtained *in situ* in liquid environment cells in the course of electrochemical cycling. For electron diffraction, the beam can be kept at low intensity, reducing

the radiolysis effects of the beam on the electrolyte. The effect of the beam on the different electrolytes has been thoroughly studied in literature, and the LiPF<sub>6</sub> EC/DMC electrolyte (used in the current paper) was shown to result in the appearance of nanoparticles after one minute exposure time, due to the decomposition of the lithium salts.<sup>49,61</sup> In the case of the electrochemical cell, where partial evaporation by the beam was necessary to obtain a thinner layer of fluid and observable reflections, we indeed saw the appearance of such nanoparticles. We did not see any ring patterns nor reflections that could originate from these nanoparticles on our electron diffraction patterns, meaning they are either amorphous or do not scatter strong enough to be seen next to the reflections originating from FePO<sub>4</sub>. Our experiment clearly shows that the resulting charged structure (FePO<sub>4</sub>) corresponds very well to that found in literature with other techniques, and thus that our result is not affected. We propose that the radiolysis does not noticeably interfere with electron diffraction tomography experiments on crystals several hundred nm in size. Possibly, only the surface layer is affected, and the surface layer contributes only marginally to the intensities of the reflections compared to the much larger volume of the bulk.

In future experiments, continuous acquisition of electron diffraction patterns should allow to track the structural changes for a single particle throughout the charge-discharge cycles. In the continuous acquisition mode, the data can be acquired within a few minutes (as compared to about an hour for the manual experiment used in the current experiment), reducing contamination and possible radiolysis. Datasets can then be obtained at different states of charge, before the accumulated contamination will significantly decrease the signal-to-noise ratio. Although this fast acquisition technique is already used in literature<sup>57-59</sup>, we could not use this method in our demonstration experiment as it needs a possibility to tilt continuously at a steady

speed without having to reposition the crystal, not available at the TEM facility used, while taking a burst of photographs using a fast camera/detector. Although numerous electrode materials have been studied *in situ* using powder diffraction with synchrotron and/or neutron radiation sources, electron diffraction tomography offers the unique possibility to perform *in situ* single crystal diffraction studies, owing to submicron crystal size which maintains its electrochemical activity. Indeed, achieving uniform delithiation for large single crystals would be impossible within reasonable time (for instance, chemical delithiation of a mm-sized  $\text{LiFePO}_4$  single crystal for 100 h results only in  $\sim 22$  mm delithiated  $\text{FePO}_4$  layer)<sup>60</sup>. Electron diffraction also has a good sensitivity towards lithium, for which otherwise neutron diffraction experiments are required. According to the Vainshtein's criterion of "light" atom detectability<sup>52</sup>, the advantage of electron diffraction compared to X-ray diffraction scales as  $\frac{w_{ED}}{w_{XRD}} = \sqrt{\frac{Z_{light}}{Z_{heavy}}}$ , where  $Z$  is the atomic number, making detection and refinement of the occupancy for "light" atoms such as Li more reliable with electron diffraction. This allows to closely follow the stepwise introduction of Li into the structure upon discharging, as demonstrated *ex situ* for  $(\text{K,Li})\text{VPO}_4\text{F}$ <sup>42</sup>. Collecting *in situ* diffraction datasets from the same single crystal at different states of charge would enable quantification of defects (as already successfully done *ex situ* for antisite defects<sup>7</sup> and stacking faults<sup>53</sup>).

Combining precession electron diffraction with *in situ* EDT experiments<sup>50,51</sup> will further improve the quality of crystallographic information as it will allow taking into account dynamical diffraction contribution intrinsic in electron diffraction. However, performing such experiments will require an electrochemical holder to be present next to the precession electron diffraction attachment in the same microscope, a rare experimental setup. However, in the case of lithium-ion battery cathodes comprising 3d transition metals as the "heaviest" elements the

dynamical effects are not very severe and kinematic refinement (as used in the current paper) is sufficient to retrieve reliable information.<sup>43</sup>

Also the use of very sensitive cameras and direct electron detectors with high dynamic ranges can further increase the signal-to-noise ratio, allowing shorter exposure times while collecting more reflections, thus further improving the quality of the refinement while decreasing the beam damage effects. An electrochemical cell with considerably less space between the windows, and thus a thinner liquid layer, would also improve the acquisition of the electron diffraction data and would allow to work without the need for evaporating part of the liquid by the beam. However, currently, no such cells are commercially available.

In conclusion, we have demonstrated that electron diffraction tomography data can be successfully collected in the *in situ* regime in an electrochemical cell with liquid electrolyte, mimicking the Li-ion battery. The quality of the diffraction data is sufficient to detect the structural changes occurring in the positive electrode (cathode) material upon charge, including variations in the unit cell parameters, and changes in the occupancy of the Li positions and interatomic distances. This opens up numerous possibilities for the structure solution and refinement of a wide range of nanosized particles from *in situ* transmission electron microscopy experiments, ranging from battery materials to electrocatalysts, as well as any nanosized particles that undergo changes or crystallization in a liquid environment.

ASSOCIATED CONTENT

### **Supporting Information**

The following files are available free of charge:

Synthesis and experimental conditions and details of TEM experiment, crystal structure data (Supporting\_Information.pdf).

The reconstruction of reciprocal space of FePO<sub>4</sub> obtained from *in situ* electron diffraction tomography (FePO4\_reciprocal\_space.mp4)

## AUTHOR INFORMATION

### Corresponding Authors

\*J. Hadermann. E-mail: [joke.hadermann@uantwerpen.be](mailto:joke.hadermann@uantwerpen.be). Phone: +3232653245.

\*A. Demortière. E-mail: [arnaud.demortiere@energie-rs2e.com](mailto:arnaud.demortiere@energie-rs2e.com) Phone: +695760165.

### Author Contributions

All authors contributed equally to this work.

### Funding Sources

O.M. Karakulina, A.M. Abakumov and J. Hadermann acknowledge support from FWO under grant G040116N. A. Demortière wants to thank the French network on the electrochemical energy storage (RS2E), the Store-Ex Labex, for the financial support. Finally, the Fonds Européen de Développement Régional (FEDER), CNRS, Région Hauts-de-France, and Ministère de l'Education Nationale de l'Enseignement Supérieur et de la Recherche are acknowledged for funding.

### Notes

The authors declare no competing financial interest.

### ABBREVIATIONS

TEM, transmission electron microscopy; EDT, electron diffraction tomography; XRD, X-ray diffraction; ND, neutron diffraction; EELS, electron energy-loss spectroscopy.

## REFERENCES

- (1) Larcher, D.; Tarascon, J. M. *Nat. Chem.* **2015**, *7* (1), 19–29.
- (2) Gröger, O.; Gasteiger, H. A.; Suchsland, J.-P. *J. Electrochem. Soc.* **2015**, *162* (14), A2605–A2622.
- (3) Deng, D. *Energy Sci. Eng.* **2015**, *3* (5), 385–418.
- (4) Tarascon, J. M.; Armand, M. *Nature* **2001**, *414* (6861), 359–367.
- (5) Croguennec, L.; Palacin, M. R. *J. Am. Chem. Soc.* **2015**, *137* (9), 3140–3156.
- (6) Sathiya, M.; Abakumov, a M.; Foix, D.; Rouse, G.; Ramesha, K.; Saubanère, M.; Doublet, M. L.; Vezin, H.; Laisa, C. P.; Prakash, a S.; Gonbeau, D.; VanTendeloo, G.; Tarascon, J.-M. *Nat. Mater.* **2014**, *14* (2), 230–238.
- (7) Karakulina, O. M.; Khasanova, N. R.; Drozhzhin, O. A.; Tsirlin, A. A.; Hadermann, J.; Antipov, E. V.; Abakumov, A. M. *Chem. Mater.* **2016**, *28* (21), 7578–7581.
- (8) Armstrong, A. R.; Holzapfel, M.; Novák, P.; Johnson, C. S.; Kang, S.-H.; Thackeray, M. M.; Bruce, P. G. *J. Am. Chem. Soc.* **2006**, *128* (26), 8694–8698.
- (9) Mikhailova, D.; Karakulina, O. M.; Batuk, D.; Hadermann, J.; Abakumov, A. M.; Herklotz, M.; Tsirlin, A. A.; Oswald, S.; Giebeler, L.; Schmidt, M.; Eckert, J.; Knapp, M.; Ehrenberg, H. *Inorg. Chem.* **2016**, *55* (14), 7079–7089.
- (10) Grey, C. P.; Tarascon, J. M. *Nat. Mater.* **2016**, *16* (1), 45–56.
- (11) Conder, J.; Marino, C.; Novák, P.; Villevieille, C. *J. Mater. Chem. A* **2018**, *6* (8), 3304–3327.
- (12) Lim, J.; Li, Y.; Alsem, D. H.; So, H.; Lee, S. C.; Bai, P.; Cogswell, D. A.; Liu, X.; Jin, N.; Yu, Y.; Salmon, N. J.; Shapiro, D. A.; Bazant, M. Z.; Tyliszczak, T.; Chueh, W. C. *Science* (80-. ). **2016**, *353* (6299), 566–571.

- (13) Yuan, Y.; Amine, K.; Lu, J.; Shahbazian-Yassar, R. *Nat. Commun.* **2017**, *8* (May), 1–14.
- (14) Lu, J.; Wu, T.; Amine, K. *Nat. Energy* **2017**, *2* (3), 17011.
- (15) Lutz, L.; Dachraoui, W.; Demortière, A.; Johnson, L. R.; Bruce, P. G.; Grimaud, A.; Tarascon, J.-M. *Nano Lett.* **2018**, *18* (2), 1280–1289.
- (16) Dachraoui, W.; Kurkulina, O.; Hadermann, J.; Demortière, A. *Microsc. Microanal.* **2016**, *22* (S5), 24–25.
- (17) Holtz, M. E.; Yu, Y.; Gunceler, D.; Gao, J.; Sundararaman, R.; Schwarz, K. A.; Arias, T. A.; Abruña, H. D.; Muller, D. A. *Nano Lett.* **2014**, *14* (3), 1453–1459.
- (18) Zeng, Z.; Liang, W.-I.; Liao, H.-G.; Xin, H. L.; Chu, Y.-H.; Zheng, H. *Nano Lett.* **2014**, *14* (4), 1745–1750.
- (19) Kolb, U.; Gorelik, T.; Kübel, C.; Otten, M. T.; Hubert, D. *Ultramicroscopy* **2007**, *107* (6–7), 507–513.
- (20) Kolb, U.; Mugnaioli, E.; Gorelik, T. E. *Cryst. Res. Technol.* **2011**, *46* (6), 542–554.
- (21) *Liquid Cell Electron Microscopy*; Ross, F. M., Ed.; Cambridge University Press: Cambridge, 2017.
- (22) Ross, F. M. *IBM J. Res. Dev.* **2000**, *44* (4), 489–501.
- (23) Williamson, M. J.; Tromp, R. M.; Vereecken, P. M.; Hull, R.; Ross, F. M. *Nat. Mater.* **2003**, *2* (8), 532–536.
- (24) Gu, M.; Parent, L. R.; Mehdi, B. L.; Unocic, R. R.; McDowell, M. T.; Sacci, R. L.; Xu, W.; Connell, J. G.; Xu, P.; Abellan, P.; Chen, X.; Zhang, Y.; Perea, D. E.; Evans, J. E.; Lauhon, L. J.; Zhang, J. G.; Liu, J.; Browning, N. D.; Cui, Y.; Arslan, I.; Wang, C. M. *Nano Lett.* **2013**, *13* (12), 6106–6112.
- (25) Unocic, R. R.; Sacci, R. L.; Brown, G. M.; Veith, G. M.; Dudney, N. J.; More, K. L.;

- Walden, F. S.; Gardiner, D. S.; Damiano, J.; Nackashi, D. P. *Microsc. Microanal.* **2014**, *20* (2), 452–461.
- (26) Wu, F.; Yao, N. *Nano Energy* **2015**, *11*, 196–210.
- (27) Holtz, M. E.; Yu, Y.; Gao, J.; Abruña, H. D.; Muller, D. A. *Microsc. Microanal.* **2013**, *19* (4), 1027–1035.
- (28) Dukes, M. J.; Jacobs, B. W.; Morgan, D. G.; Hegde, H.; Kelly, D. F. *Chem. Commun.* **2013**, *49* (29), 3007–3009.
- (29) Jungjohann, K. L.; Evans, J. E.; Aguiar, J. A.; Arslan, I.; Browning, N. D. *Microsc. Microanal.* **2012**, *18* (3), 621–627.
- (30) Nielsen, M. H.; Aloni, S.; De Yoreo, J. J. *Science (80-. )*. **2014**, *345* (6201), 1158–1162.
- (31) Smeets, P. J. M.; Cho, K. R.; Kempen, R. G. E.; Sommerdijk, N. A. J. M.; De Yoreo, J. J. *Nat. Mater.* **2015**, *14* (4), 394–399.
- (32) White, E. R.; Singer, S. B.; Augustyn, V.; Hubbard, W. A.; Mecklenburg, M.; Dunn, B.; Regan, B. C. *ACS Nano* **2012**, *6* (7), 6308–6317.
- (33) Unocic, R. R.; Baggetto, L.; Veith, G. M.; Aguiar, J. A.; Unocic, K. A.; Sacci, R. L.; Dudney, N. J.; More, K. L. *Chem. Commun.* **2015**, *51* (91), 16377–16380.
- (34) Kolb, U.; Gorelik, T.; Otten, M. T. *Ultramicroscopy* **2008**, *108* (8), 763–772.
- (35) Zhang, Y.; Su, J.; Furukawa, H.; Yun, Y.; Gándara, F.; Duong, A.; Zou, X.; Yaghi, O. M. *J. Am. Chem. Soc.* **2013**, *135* (44), 16336–16339.
- (36) Su, J.; Kapaca, E.; Liu, L.; Georgieva, V.; Wan, W.; Sun, J.; Valtchev, V.; Hovmöller, S.; Zou, X. *Microporous Mesoporous Mater.* **2014**, *189*, 115–125.
- (37) Boullay, P.; Palatinus, L.; Barrier, N. *Inorg Chem* **2013**, *52*, 8–10.
- (38) Colmont, M.; Palatinus, L.; Huvé, M.; Kabbour, H.; Saitzek, S.; Djelal, N.; Roussel, P.

- Inorg. Chem.* **2016**, *55* (5), 2252–2260.
- (39) Palatinus, L.; Klementová, M.; Dřínek, V.; Jarošová, M.; Petříček, V. *Inorg. Chem.* **2011**, *50* (8), 3743–3751.
- (40) Sun, Q.; Ma, Y.; Wang, N.; Li, X.; Xi, D.; Xu, J.; Deng, F.; Yoon, K. B.; Oleynikov, P.; Terasaki, O.; Yu, J. *J. Mater. Chem. A* **2014**, *2* (42), 17828–17839.
- (41) Yun, Y.; Zou, X.; Hovmöller, S.; Wan, W. *IUCrJ* **2015**, *2*, 267–282.
- (42) Fedotov, S. S.; Khasanova, N. R.; Samarin, A. S.; Drozhzhin, O. A.; Batuk, D.; Karakulina, O. M.; Hadermann, J.; Abakumov, A. M.; Antipov, E. V. *Chem. Mater.* **2016**, *28* (2), 411–415.
- (43) Drozhzhin, O. A.; Sumanov, V. D.; Karakulina, O. M.; Abakumov, A. M.; Hadermann, J.; Baranov, A. N.; Stevenson, K. J.; Antipov, E. V. *Electrochim. Acta* **2016**, *191*, 149–157.
- (44) Roberts, M.; Biendicho, J. J.; Hull, S.; Beran, P.; Gustafsson, T.; Svensson, G.; Edström, K. *J. Power Sources* **2013**, *226*, 249–255.
- (45) Ring, E. A.; de Jonge, N. *Micron* **2012**, *43* (11), 1078–1084.
- (46) Palatinus, L. *PETS—program for analysis of electron diffraction data*; Institute of Physics: Prague, Czech Republic, 2011.
- (47) Petříček, V.; Dušek, M.; Palatinus, L. *Zeitschrift für Krist.* **2014**, *229* (5), 345–352.
- (48) Palatinus, L.; Chapuis, G. *J. Appl. Crystallogr.* **2007**, *40* (4), 786–790.
- (49) Abellan, P.; Mehdi, B. L.; Parent, L. R.; Gu, M.; Park, C.; Xu, W.; Zhang, Y.; Arslan, I.; Zhang, J.-G.; Wang, C.-M.; Evans, J. E.; Browning, N. D. *Nano Lett.* **2014**, *14* (3), 1293–1299.
- (50) Palatinus, L.; Petříček, V.; Corrêa, C. A. *Acta Crystallogr. Sect. A Found. Adv.* **2015**, *71* (2), 235–244.

- (51) Palatinus, L.; Corrêa, C. A.; Steciuk, G.; Jacob, D.; Roussel, P.; Boullay, P.; Klementová, M.; Gemmi, M.; Kopeček, J.; Domeneghetti, M. C.; Cámara, F.; Petříček, V. *Acta Crystallogr. Sect. B Struct. Sci. Cryst. Eng. Mater.* **2015**, *71* (6), 740–751.
- (52) Vainshtein, B. K.; Zvyagin, B. B.; Avilov, A. S. In *Electron Diffraction Techniques* (ed. J.M. Cowley), 1993
- (53) Zhao, H. ; Krysiak, Y. ; Hoffmann, K. ; Barton, B. ; Molina-Luna, L.; Neder, R.B. ; Kleebe, H.J. ; Gesing, T.M. ; Schneider, H. ; Fischer, R.X.; Kolb, U. *J. Solid State Chem.* **2017**, *249*, 114–123.
- (54) Nayak, P. K.; Erickson, E. M.; Schipper, F.; Penki, T. R.; Munichandraiah, N.; Adelhelm, P.; Sclar, H.; Amalraj, F.; Markovsky, B.; Aurbach, D. *Adv. Energy Mater.* **2017**, *1702397*, 1702397.
- (55) Pimenta, V.; Sathiya, M.; Batuk, D.; Abakumov, A. M.; Giaume, D.; Cassaignon, S.; Larcher, D.; Tarascon, J. M. *Chem. Mater.* **2017**, *29* (23), 9923–9936.
- (56) Kleiner, K.; Strehle, B.; Baker, A. R.; Day, S. J.; Tang, C. C.; Buchberger, I.; Chesneau, F.-F.; Gasteiger, H. A.; Piana, M. *Chem. Mater.* **2018**, *30* (11), 3656–3667.
- (57) Simancas, J.; Simancas, R.; Bereciartua, P. J.; Jorda, J. L.; Rey, F.; Corma, A.; Nicolopoulos, S.; Pratim Das, P.; Gemmi, M.; Mugnaioli, E. *J. Am. Chem. Soc.* **2016**, *138* (32), 10116–10119
- (58) Van Genderen, E.; Clabbers, M. T. B.; Das, P. P.; Stewart, A.; Nederlof, I.; Barentsen, K. C.; Portillo, Q.; Pannu, N. S.; Nicolopoulos, S.; Gruene, T.; Abrahams, J.P. *Acta Crystallogr. Sect. A Found. Adv.* **2016**, *72*, 236–242.
- (59) Gemmi, M.; La Placa, M. G. I.; Galanis, A. S.; Rauch, E. F.; Nicolopoulos, S. *J. Appl. Crystallogr.* **2015**, *48* (i), 718–727.

- (60) Weichert, K ; Sigle, W ; van Aken, P.A. ; Jamnik, J. ; Zhu, C. ; Amin, R. ; Acartuřrk, T. ; Starke, U. ; Maier, J. *J. Am. Chem.Soc.* **2012**, *134*, 2988–2992.
- (61) Li, Y.; Li, Y.; Pei, A.; Yan, K.; Sun, Y.; Wu, C.-L.; Joubert, L.-M.; Chin, R.; Koh, A. L.; Yu, Y.; Perrino, J. ; Butz, B. ; Chu, S. ; Cui, Y.*Science* **2017**, *358*, 506–510.

## Table of Contents Graphic

